Annals of Biomedical Engineering, Vol. 42, No. 9, September 2014 (© 2014) pp. 1853–1866
DOI: 10.1007/s10439-014-1054-0

Passive Stiffness of Coupled Wrist and Forearm Rotations

WILL B. DRAKE[1] and STEVEN K. CHARLES[2]

[1]Department of Mechanical Engineering, Brigham Young University, Provo, UT 84602, USA; and [2]Department of Mechanical Engineering and Neuroscience Center, Brigham Young University, 435 CTB, Provo, UT 84602, USA

(*Received 23 September 2013; accepted 3 June 2014; published online 8 June 2014*)

Associate Editor Michael R. Torry oversaw the review of this article.

Abstract—Coordinated movement requires that the neuromuscular system account and compensate for movement dynamics. One particularly complex aspect of movement dynamics is the interaction that occurs between degrees of freedom (DOF), which may be caused by inertia, damping, and/or stiffness. During wrist rotations, the two DOF of the wrist (flexion–extension and radial–ulnar deviation, FE and RUD) are coupled through interaction torques arising from passive joint stiffness. One important unanswered question is whether the DOF of the forearm (pronation–supination, PS) is coupled to the two DOF of the wrist. Answering this question, and understanding the dynamics of wrist and forearm rotations in general, requires knowledge of the stiffness encountered during rotations involving all three DOF (PS, FE, and RUD). Here we present the first-ever measurement of the passive stiffness encountered during simultaneous wrist and forearm rotations. Using a wrist and forearm robot, we measured coupled wrist and forearm stiffness in 10 subjects and present it as a 3-by-3 stiffness matrix. This measurement of passive wrist and forearm stiffness will enable future studies investigating the dynamics of wrist and forearm rotations, exposing the dynamics for which the neuromuscular system must plan and compensate during movements involving the wrist and forearm.

Keywords—Interaction, Dynamics, Motor control, Pronation, Supination.

LIST OF ABBREVIATIONS

DOF	Degree(s) of freedom
sEMG	Surface electromyogram
FE	Flexion–extension of the wrist
MVC	Maximum voluntary contraction
PS	Pronation–supination of the forearm
RUD	Radial–ulnar deviation of the wrist

Address correspondence to Steven K. Charles, Department of Mechanical Engineering and Neuroscience Center, Brigham Young University, 435 CTB, Provo, UT 84602, USA. Electronic mail: skcharles@byu.edu

INTRODUCTION

Coordinated motor control requires that the neuromuscular system account and compensate for joint dynamics. For example, during reaching movements, inertial interaction torques couple the shoulder and elbow, creating a torque about the elbow in response to a rotation about the shoulder, and vice versa.[20] Decades of motor control studies have investigated how the neuromuscular system plans and compensates for these complex inertial dynamics.

Coordinated wrist rotations also involve complex dynamics, but in contrast to reaching movements, wrist rotations are dominated by stiffness, not inertia; the torque required to overcome the passive stiffness (i.e., in the absence of muscle activity) of the wrist during comfortably paced wrist rotations is approximately ten times larger than the torque required to overcome the inertia of the hand.[8] Furthermore, because the passive stiffness of the wrist is anisotropic, with greater stiffness in radial–ulnar deviation (RUD) than in flexion–extension (FE), and does not align with the anatomical axes of the wrist,[14] the two degrees of freedom (DOF) of the wrist (FE and RUD) are coupled through interaction torques arising from stiffness.[8] Very few studies have investigated how the neuromuscular system plans and compensates for the interaction due to joint stiffness, and many unanswered questions remain.

An important unanswered question is whether forearm rotations (pronation–supination, PS) are coupled through joint stiffness to wrist rotations. Wrist and forearm rotations often occur together,[2] but the passive dynamics of simultaneous wrist and forearm rotations are currently unknown. Consequently, we also do not know what the neuromuscular system has to plan and compensate for in order to make coordinated movements involving the wrist and forearm.

Understanding the dynamics of wrist and forearm rotations, and in particular whether the wrist and forearm are coupled, requires knowledge of the passive stiffness encountered during rotations involving all three DOF (PS, FE, and RUD) *simultaneously*. Measurements of stiffness in each DOF individually, or even in two DOF simultaneously, are not sufficient to characterize the dynamics of movements involving all three DOF. However, most previous studies of wrist or forearm stiffness have measured passive joint stiffness in only 1 DOF, most often FE.[3,12,17,24,25] Few studies have measured stiffness in RUD,[28] and only one study has measured stiffness in combinations of FE and RUD.[14] Likewise, few studies have measure the passive stiffness in PS.[14] No study has measured the passive stiffness involving all three DOF.

Here we present the first-ever measurement of the passive stiffness encountered during movements involving simultaneous wrist and forearm rotations. We measured the torque–displacement relationship while the wrist and forearm were passively rotated from neutral position through 15° rotations involving combinations of PS, FE, and RUD, and used multiple linear regression to determine from that relationship the stiffness, presented as a 3-by-3 stiffness matrix. This measurement of passive wrist and forearm stiffness will enable future studies to investigate the dynamics of wrist and forearm rotations, exposing the dynamics for which the neuromuscular system must plan and compensate during movements involving the wrist and forearm.

METHODS

Subjects

Ten right-handed subjects [five female, 24 ± 5.42 years old (mean ± SD), range 18–38 years] with no history of neurological or biomechanical disorders affecting the wrist and forearm were recruited for the study. Because strenuous exercise may have a significant effect on passive joint stiffness,[24,27,29,30] subjects were instructed to refrain from strenuous upper body exercise for the 48 h period preceding the study. Each subject gave informed consent consistent with the procedures outlined by BYU's Institutional Review Board.

Experimental Setup

An InMotion Wrist Rehabilitation Robot (Interactive Motion Technologies, MA) was used to measure stiffness. This robot is capable of moving the wrist and forearm independently in PS, FE, and RUD, senses displacement in each DOF at 200 Hz with a resolution of 0.0006°, and is able to apply 1.95 N m of torque in FE and RUD and 2.10 N m of torque in PS.[22] Subjects were seated at the robot with the right arm in the parasagittal plane, the shoulder in 0° abduction, approximately 15° flexion, and 0° humeral rotation, and with the elbow in approximately 30° of flexion.

We aligned each subject's PS axis with the robot's PS axis as follows. The PS stage of the robot was designed to approximately coincide with the average user's PS axis when his/her forearm is placed on the robot's PS stage.[31] We placed the medial aspect of each subject's forearm on the PS stage of the robot and adjusted the height of the robot as necessary to place the long axis of the forearm approximately in the same horizontal plane as the PS axis of the robot. The dorsal aspect of the distal forearm was strapped to a plate attached to the robot's PS stage (Fig. 1), which placed the forearm in approximately the same parasagittal plane as the PS axis of the robot. Thus, the offset between the PS axes of the forearm and robot was approximately zero.

Attaching the dorsal aspect of the distal forearm to the plate (Fig. 1) oriented the FE axis of the wrist, which was assumed to be perpendicular to the PS axis of the forearm and parallel to the dorsal aspect of the distal forearm, parallel to the FE axis of the robot because this latter axis was itself parallel with the plate. We assumed the location of the FE axis of the wrist to be at the wrist joint center, located by external palpation using the following method, which is similar to the method validated by An *et al.*[1] The proximodistal and mediolateral location of the wrist joint center was palpated on the dorsal aspect of the hand and wrist and was assumed to be halfway between the distal end of the radius and the proximal end of the third metacarpal, and halfway between the medial and lateral aspects of the wrist. The ventrodorsal location of the wrist joint center was assumed to be halfway between the ventral and dorsal aspects of the wrist. We aligned the location of the FE axis of the wrist with that of the robot as well as possible, but the location of the robot's differential gear mechanism under the wrist (Fig. 1) forces the FE axis of the wrist to be slightly distal to the FE axis of the robot to avoid the medial aspect of the subject's hand pressing against the housing covering the robot's differential gear mechanism, which would artificially increase the torque and therefore the stiffness measurement. The offset between the two parallel FE axes was approximately 2 cm.

This alignment placed the RUD axis of the wrist, which was assumed to be perpendicular to both the PS of the forearm and the FE axis of the wrist, parallel to the RUD axis of the robot because this latter axis is perpendicular to the PS and FE axes of the robot. The

RUD axis of the wrist was assumed to intersect with the FE axis of the wrist at the wrist joint center. While the actual FE and RUD axes do not intersect perfectly, the offset between the axes is small and has been shown to have a negligible effect on wrist joint dynamics.[8] The robot was designed with extra DOF,[31] including the linear bearing and the revolute joint that attaches it to the rest of the robot (Fig. 1), to allow an offset of approximately 8 cm between the RUD axes of the wrist and robot, and to follow the RUD angle of the wrist with a ratio of approximately 1 despite this offset (see "Discussion" section).

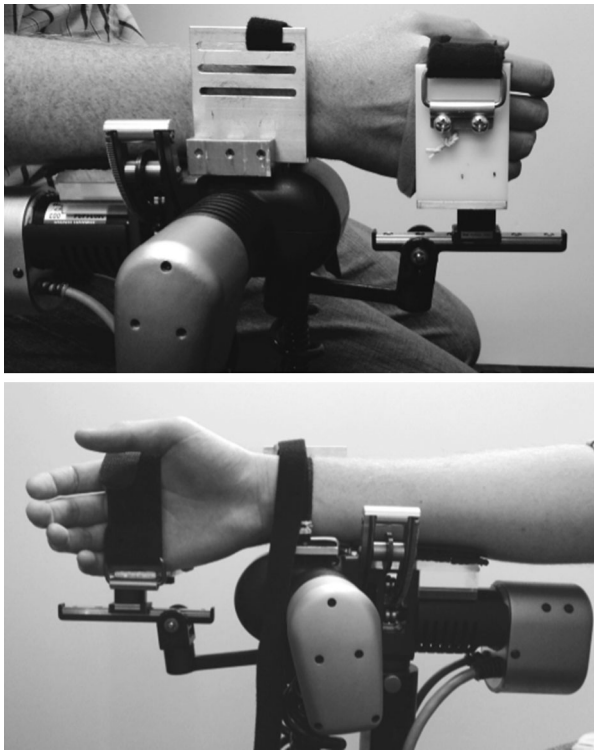

FIGURE 1. The custom interface used to attach the subject's forearm and hand to the robot. The interface secured the distal forearm to the PS stage of the robot and the hand to the FE–RUD stage of the robot. The interface at the hand attached to the metacarpals (instead of requiring the subject to grasp a handle), allowing forearm, wrist, and hand muscles to relax and leaving the fingers unconstrained.

The robot manipulated the subjects' right wrist and forearm *via* a custom interface attached to the subjects' right hand (Fig. 1). Because active gripping increases wrist stiffness through muscle activation and because finger constraint has been demonstrated to have a significant effect on the wrist's range of motion,[16] the custom interface attached to the subject's hand along the palmar and dorsal aspects of the metacarpals, obviating the need for the subject to grip a handle and leaving the fingers unconstrained (Fig. 1). Each subject's distal forearm was attached with straps to the PS stage of the robot.

Protocol

We measured stiffness throughout the range extending ±15° from neutral position (defined below) in discrete movements combining PS, FE, and RUD. We chose ±15° because wrist stiffness was previously shown to be relatively constant over this range.[14] The robot rotated the forearm and wrist between neutral position and 134 targets equally distributed on the surface of a sphere of radius 15° in PS–FE–RUD space (Fig. 2). More specifically, the targets were uniformly distributed in spherical coordinates, with azimuth (in the FE–RUD plane) ranging from 0 to 2π and elevation (along the PS axis) ranging from 0 to π, and converted to Cartesian coordinates.

When muscle is stretched more than 1% of its length from rest, the stiffness during the initial portion of the movement is significantly higher than during the rest of the movement.[5] For the wrist, this short-range-stiffness effect has been observed over the initial 3°–4° of wrist rotation.[3] To allow us to later remove this

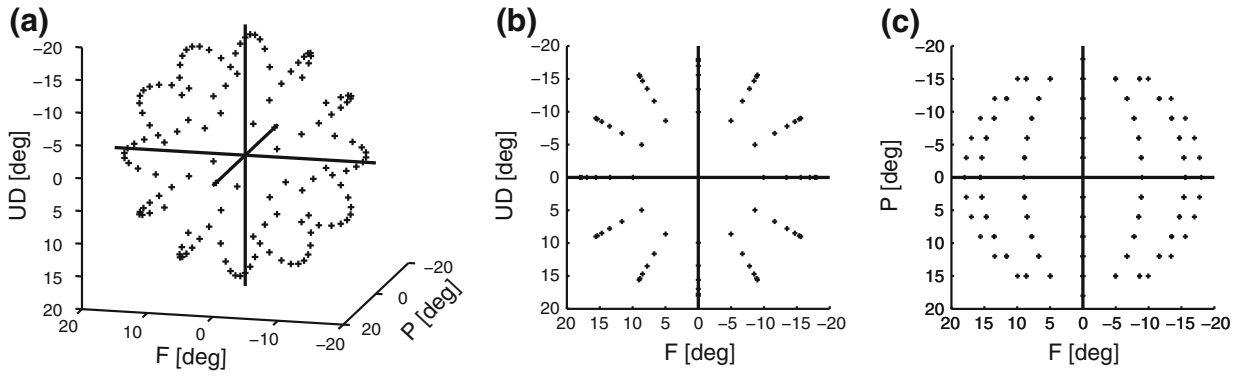

FIGURE 2. The robot was programed to move from neutral position (origin) to each of these 134 positions in PS–FE–RUD space. (a) Isometric view. (b) The 12 divisions in FE–RUD space. (c) The 13 divisions along the PS axis (the distribution in PS–RUD space is identical). Negative pronation, flexion, and ulnar deviation represent supination, extension, and radial deviation, respectively).

short-range stiffness effect, additional 3° bands were added to the beginning and end of each movement. The resulting outbound movement was programed to begin at −3° relative to the neutral position, pass through the neutral position, and end at +18° relative to neutral position. The inbound movement extended from +18° through the origin to −3°. The robot was commanded *via* proportional-derivative control, with proportional and derivative gains of 10.0 N m/rad and 0.1 N m s/rad for FE and RUD, and gains of 20.0 N m/rad and 0.3 N m s/rad for PS. By this control scheme, the actual displacement was generally less than the commanded displacement by approximately 20%. Each movement was repeated three times in succession before proceeding to the next target. The session lasted a total of 50 min.

Subjects were instructed to relax their upper arm as much as possible during the duration of the session. To minimize the likelihood of stimulating reflexes, the robot was programed to move slowly and smoothly following a minimum jerk trajectory with average velocity of 5.2°/s. Measurements of wrist stiffness were previously shown to be insensitive to movement velocity when the average velocity was below 12°/s.[14] We verified that muscles were relaxed by recording muscle activity with surface electromyogram (sEMG) sensors (Trigno by Delsys, Boston, MA) at 200 Hz during each session. While under-sampling sEMG is not advisable in general, we only used it to calculate the average amplitude, which is relatively unaffected by under-sampling.[21,23] The sEMG sensors were placed over the flexor carpi radialis, flexor carpi ulnaris, extensor carpi radialis, extensor carpi ulnaris, pronator teres, and biceps. The biceps was selected because it is the supination muscle most accessible by sEMG. Following completion of the session, three sets of maximum voluntary contraction (MVC) sEMG measurements were obtained.

Neutral position was defined similar to ISB recommendations for global movements,[32] with the following approximations for *in vivo* use. The forearm was in neutral PS when the dorsal aspect of the distal forearm, more specifically the dorsal tubercle of the radius and the dorsal-most protuberance of the ulnar head, was parallel to the vertical plane containing the arm and forearm. FE and RUD were defined to be in neutral position when the long axis of the third metacarpal aligned with the long axis of the forearm.[32] The wrist was in neutral FE and RUD when the elbow joint center, the wrist joint center, and the center of the head of the third metacarpal were aligned. The subject was placed in the neutral position by changing the zero position of the robot.

Data Processing

The wrist robot output included joint torques, which were calculated from motor voltages, and actual displacements in FE, RUD, and PS. All torque–displacement relationships showed the hysteresis loops commonly observed in connective tissue, including muscle,[15] and which have been previously observed in upper limb joints.[14,18] Hysteresis manifests as a sudden change in torque when the direction of movement is reversed. To remove this non-linear effect, we separated the data into outbound and inbound movements and shifted outbound torques and displacements to begin at the origin, and inbound torques and displacements to end at the origin. This was done after removing the short-range stiffness effects, which were observed primarily in the first 2° of movement. By removing the discontinuity due to hysteresis, this translation facilitated the multiple linear regression described below without affecting the slope (i.e., stiffness) of any particular movement.

The torque–displacement data formed a vector field of torques, $\vec{\tau}(\theta_{PS}, \theta_{FE}, \theta_{RUD})$, at different values of PS, FE, and RUD (θ_{PS}, θ_{FE}, and θ_{RUD}). The 3-DOF stiffness matrix K was derived by linearizing the torque vector $\vec{\tau}$ by Taylor series expansion:

$$\begin{bmatrix} \tau_{PS} \\ \tau_{FE} \\ \tau_{RUD} \end{bmatrix} = \begin{bmatrix} \frac{\partial \tau_{PS}}{\partial \theta_{PS}}\theta_{PS} + \frac{\partial \tau_{PS}}{\partial \theta_{FE}}\theta_{FE} + \frac{\partial \tau_{PS}}{\partial \theta_{RUD}}\theta_{RUD} \\ \frac{\partial \tau_{FE}}{\partial \theta_{PS}}\theta_{PS} + \frac{\partial \tau_{FE}}{\partial \theta_{FE}}\theta_{FE} + \frac{\partial \tau_{FE}}{\partial \theta_{RUD}}\theta_{RUD} \\ \frac{\partial \tau_{RUD}}{\partial \theta_{PS}}\theta_{PS} + \frac{\partial \tau_{RUD}}{\partial \theta_{FE}}\theta_{FE} + \frac{\partial \tau_{RUD}}{\partial \theta_{RUD}}\theta_{RUD} \end{bmatrix}$$

$$= \begin{bmatrix} \frac{\partial \tau_{PS}}{\partial \theta_{PS}} & \frac{\partial \tau_{PS}}{\partial \theta_{FE}} & \frac{\partial \tau_{PS}}{\partial \theta_{RUD}} \\ \frac{\partial \tau_{FE}}{\partial \theta_{PS}} & \frac{\partial \tau_{FE}}{\partial \theta_{FE}} & \frac{\partial \tau_{FE}}{\partial \theta_{RUD}} \\ \frac{\partial \tau_{RUD}}{\partial \theta_{PS}} & \frac{\partial \tau_{RUD}}{\partial \theta_{FE}} & \frac{\partial \tau_{RUD}}{\partial \theta_{RUD}} \end{bmatrix} \begin{bmatrix} \theta_{PS} \\ \theta_{FE} \\ \theta_{RUD} \end{bmatrix}$$

$$= \begin{bmatrix} K_{PS,PS} & K_{PS,FE} & K_{PS,RUD} \\ K_{FE,PS} & K_{FE,FE} & K_{FE,RUD} \\ K_{RUD,PS} & K_{RUD,FE} & K_{RUD,RUD} \end{bmatrix} \begin{bmatrix} \theta_{PS} \\ \theta_{FE} \\ \theta_{RUD} \end{bmatrix}$$

$$= K \begin{bmatrix} \theta_{PS} \\ \theta_{FE} \\ \theta_{RUD} \end{bmatrix}$$

The subject-specific values for each row of the total measured stiffness matrix K were computed by multiple linear regression using Matlab's regress function:

$$[\,K_{PS,PS} \quad K_{PS,FE} \quad K_{PS,RUD}\,] = \text{regress}(\tau_{PS}, [\,1 \quad \theta_{PS} \quad \theta_{FE} \quad \theta_{RUD}\,])$$
$$[\,K_{FE,PS} \quad K_{FE,FE} \quad K_{FE,RUD}\,] = \text{regress}(\tau_{FE}, [\,1 \quad \theta_{PS} \quad \theta_{FE} \quad \theta_{RUD}\,])$$
$$[\,K_{RUD,PS} \quad K_{RUD,FE} \quad K_{RUD,RUD}\,] = \text{regress}(\tau_{RUD}, [\,1 \quad \theta_{PS} \quad \theta_{FE} \quad \theta_{RUD}\,])$$

The measured robot torques do not originate solely from passive joint stiffness, but represent the sum of torques from (1) passive wrist stiffness, (2) mechanical impedance in the robot, and (3) apparent stiffness due to gravity. Consequently, the stiffness matrix would include apparent stiffness from all three phenomena and not the passive wrist stiffness only. Therefore, we removed the two latter effects in the following manner. A stiffness compensation matrix representing only robot-based and gravity-induced effects was measured for each subject by repeating the experimental protocol with a substitute mass attached to the robot instead of the subject's hand. The substitute mass was matched to that of each subject's hand using anthropometric measurements and regression equations from de Leva,[10] and the position of the substitute mass in the robot and the neutral position of the robot were matched to each subject's condition. We then subtracted the subject-specific stiffness compensation matrix from each subject's total measured stiffness matrix to yield the passive wrist stiffness matrix.

The measured stiffness matrix contains both conservative and non-conservative components, but pure spring-like behavior is perfectly conservative.[19,26] Since for human joints the non-conservative component is generally negligible compared to the conservative component, and since only the conservative component is guaranteed to have real eigenvalues needed for representing stiffness as an ellipsoid (see below), it is common to separate the measured stiffness into its conservative (symmetric) and non-conservative (anti-symmetric) parts, and to discard the non-conservative component.[14,19] To verify that the non-conservative component was indeed negligible and could be discarded, we compared the relative sizes of the symmetric and anti-symmetric portions by comparing the sum of the magnitudes of the torques arising from either portion for 134 unit displacements equally distributed throughout PS–FE–RUD space.

All sEMG data were detrended, rectified, and low-pass filtered using a 2nd order Butterworth filter with a cutoff frequency of 3 Hz. The maximum values of processed sEMG from each of the three processed MVC data sets were averaged to establish the MVC value for each of the six sEMG signals for each subject. A subject was considered to be not relaxed if the average sEMG reading during a movement exceeded a threshold. We chose this threshold to be 6% of the individual's MVC, similar to the prior study by Formica *et al.*[14] Of the 2040 movements recorded throughout the study, 99% fell below the 6% MVC threshold. The remaining movements were excluded from the analysis.

To provide a measure of how accurately the final linear approximation predicts the raw measured torque, we calculated for each sample the difference between the raw measured torque and the torque predicted at that location by the symmetric stiffness matrix. Because the symmetric stiffness matrix does not include the effects of gravity and robot dynamics, the raw measured torque was defined as the difference between the torque measured with the subject and the torque measured with the substitute mass. We calculated the difference in the magnitude and the difference in the angle between the measured and predicted torque vectors and averaged them for the entire measurement range, the near range (within 7.5° of neutral position), and the far range (outside of 7.5° from neutral position). Movements with a difference in magnitudes beyond 3 SD from the mean were excluded. The mean and standard deviation of the difference in angle were calculated using circular statistics to account for periodicity, which defines the mean of a set of angles as the angle of the mean of unit vectors whose angles equal the set of angles, and the standard deviation as $\sqrt{2(1-R)}$, where R is the length of the mean vector.[4] This forces the standard deviation to lie on the interval between 0 and $\sqrt{2}$, with zero indicating tightly grouped angles.

Analysis

A symmetric stiffness matrix is more intuitively analyzed in terms of the shape, orientation, and volume of its stiffness ellipsoid. This ellipsoid represents the locus of torques due to stiffness caused by a unit displacement in every direction. In other words, a unit displacement in any direction produces a torque vector whose tip lies somewhere on the ellipsoid. In general, a displacement vector and the torque vector it causes are not collinear, except in the direction of the principal (major, intermediate, and minor) axes of the ellipsoid.

The directions and magnitudes of the principal axes of the stiffness ellipsoid are given by the eigenvectors and eigenvalues of the stiffness matrix, respectively.[13] We characterized the shape of the ellipsoid by the ratios of the intermediate and minor eigenvalues with respect to the major eigenvalue: λ_2/λ_1 and λ_3/λ_1,, where λ_1, λ_2, and λ_3 are the major, intermediate, and minor eigenvalues, respectively. The orientation of the ellipsoid was determined as the angles between the principal axes and the PS, FE, and RUD axes. The volume of the ellipsoid represents the overall magnitude of the passive stiffness and was calculated as $\frac{4}{3}\pi\lambda_1\lambda_2\lambda_3$.

To determine the effect of experimental conditions on stiffness, we performed four ANOVA tests, one for each of the following parameters of the stiffness ellipsoid: ratio of minor to major eigenvalue, ratio of intermediate to major eigenvalue, angle between the major axis and the RUD axis, and volume. Each test was a mixed-effects ANOVA with direction (outbound or inbound) and gender as fixed factors and subject (1–10) as a random factor.

RESULTS

Raw displacement and torque data are shown in Fig. 3 for a representative movement involving PS, FE, and RUD. The muscle activity averaged over all subjects was 0.70 ± 0.68% (mean ± SD) of MVC, with no subject exceeding an average of 1.8% MVC, indicating that subjects remained relaxed during the experiment. Consistent with previous findings,[3] we observed the short-range-stiffness phenomenon in approximately the first 2° of displacement and excluded it from the analysis, leaving an average displacement of 14.69° ± 1.04° in each direction.

The multiple linear regression showed a linear relationship between torque and displacement: the mean R^2 value for each row of the stiffness matrix before accounting for robot and gravitational effects was found to be 0.90 ± 0.04 (range 0.82–0.98). After compensating for gravity and robot dynamics, the matrices were separated into symmetric and antisymmetric parts (Fig. 4). On average, the sum of the magnitude of the resultant torques due to the antisymmetric matrix was only 3 ± 1% of that produced by the symmetric matrix, so the symmetric matrix was nearly identical to the total matrix (Fig. 4). The antisymmetric matrix was excluded from further analysis, yielding the symmetric stiffness matrices shown in Table 1 and represented in Fig. 5.

We compared the torque predicted by the stiffness matrix to the raw measured torque, defined here as the

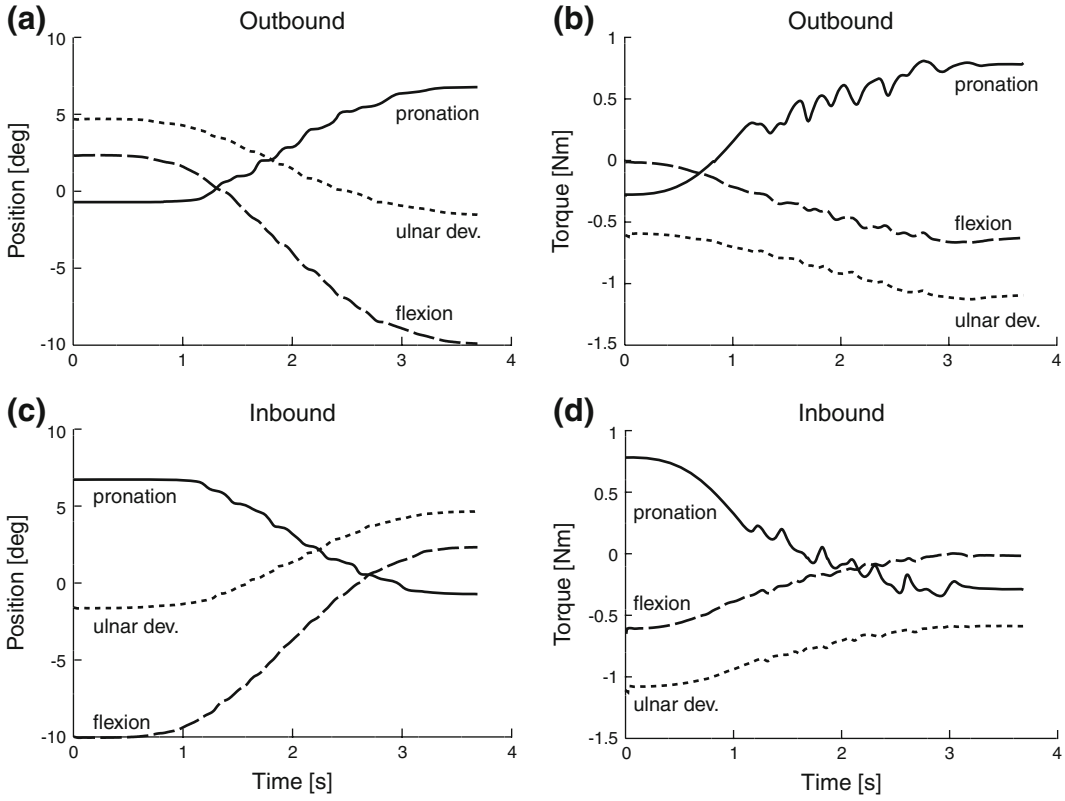

FIGURE 3. Raw displacement and torque for a representative outbound (a, b) and inbound (c, d) movement involving PS, FE, and RUD. Negative displacement and torque in pronation represent displacement and torque in supination, respectively (and similarly for flexion and ulnar deviation).

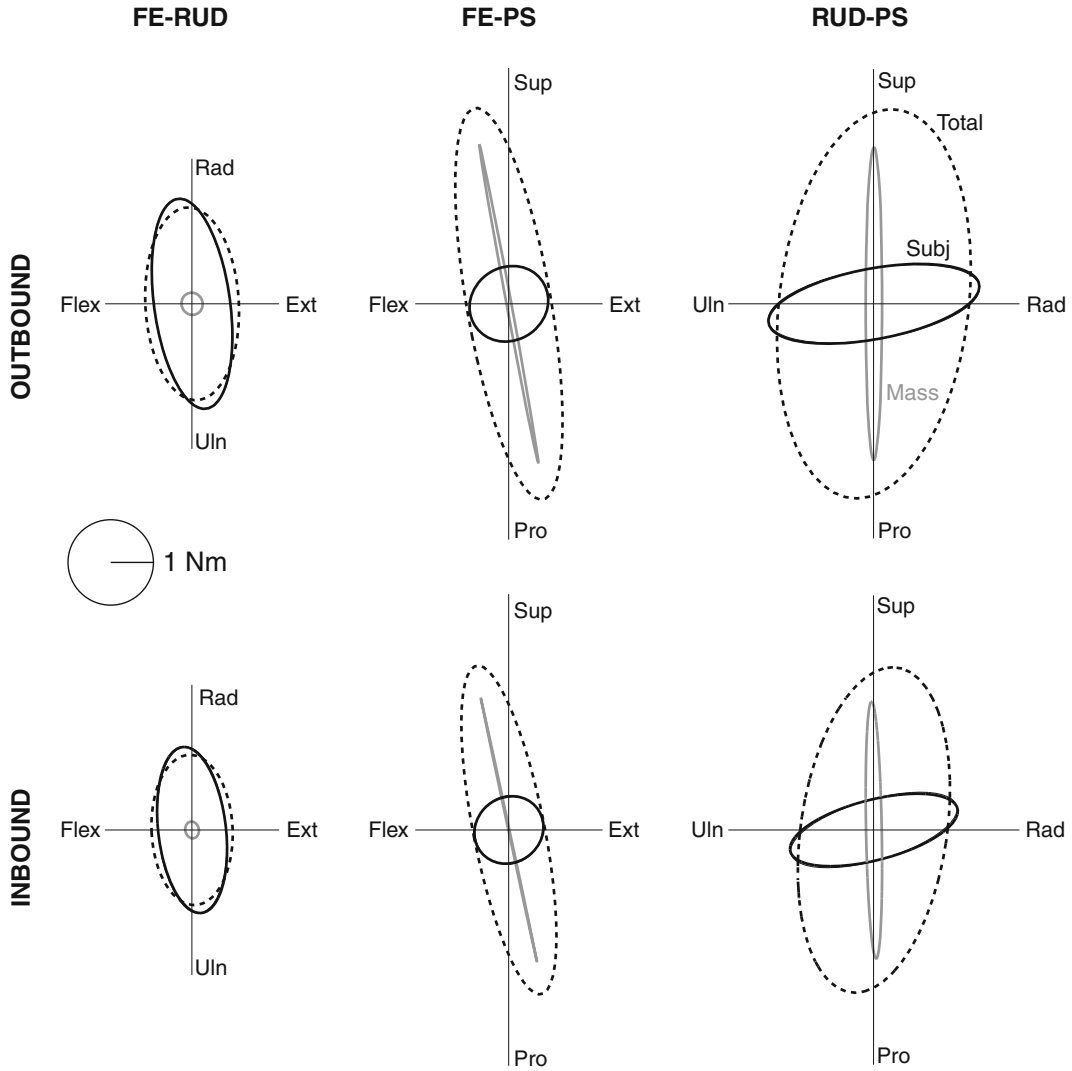

FIGURE 4. The stiffness ellipsoid at various stages of data processing for a single subject. Shown are the two-dimensional projections (i.e., ellipses) corresponding to the matrices from the measurement with the subject (''Total,'' shown dotted black); the measurement with the substitute mass (''Mass,'' shown in gray); and the difference, which represents the subject's stiffness after compensating for robot dynamics and gravitational effects (''Subj,'' shown in solid black). The conservative (symmetric) portion of the subject's stiffness is also plotted but is indistinguishable from ''Subj'' because the non-conservative (anti-symmetric) portion is so small. The apparent stiffness due to robot dynamics and gravitational effects is much larger in PS than in FE and RUD because the center of mass of the PS stage of the robot lies below the PS axis and the moment arm increases with displacement in PS. The scale for 1 N m is shown on the left (the scale has units of torque because stiffness ellipses represent the locus of torques caused by unit displacements in every direction). Pro, sup, flex, ext, uln, and rad represent pronation, supination, flexion, extension, ulnar deviation, and radial deviation, respectively.

difference between the torque measured with the subject and the torque measured with the substitute mass (Fig. 6). Averaged over all movements, the symmetric stiffness matrix underestimated the magnitude of the raw measured torque by 9.6 ± 69% (mean ± SD) over the entire range and 28 ± 58% over the region within 7.5° of neutral position, and overestimated the magnitude of the raw measured torque by 10 ± 73% over the region beyond 7.5° from neutral position (the large SD values are discussed in the ''Discussion'' section). The mean difference in angle between the measured and predicted vectors was 3.6°, 12°, and 1.2°, with angular standard deviations of 1.11, 1.29, and 0.88 (see ''Methods'' section), for the entire, near, and far regions, respectively.

The shape of the stiffness ellipsoids was highly anisotropic (Fig. 5; Table 2): on average, the ratios of intermediate to major eigenvalue and minor to major eigenvalue were 0.43 ± 0.11 and 0.21 ± 0.09, respectively, with no statistically significant effects of direction or gender on either ratio (Table 3). The ratio of minor to intermediate eigenvalue was 0.49 ± 0.17.

TABLE 1. Mean stiffness matrices and standard deviations (after compensating for robot dynamics and gravitational effects, and after removing the non-conservative portion) for subsets of the study.

	Mean (N m/rad)			SD (N m/rad)			
	P	F	U	P	F	U	R^2
Male							
Outbound							
P	0.75	0.02	0.29	0.24	0.15	0.19	0.85–0.88
F	0.02	1	−0.12	0.15	0.23	0.13	0.92–0.94
U	0.29	−0.12	3	0.19	0.13	0.9	0.92–0.97
Inbound							
P	0.7	0.03	0.28	0.21	0.12	0.16	0.86–0.88
F	0.03	0.92	−0.06	0.12	0.25	0.09	0.86–0.91
U	0.28	−0.06	2.55	0.16	0.09	0.79	0.95–0.98
Female							
Outbound							
P	0.87	0.07	0.15	0.74	0.11	0.05	0.82–0.91
F	0.07	0.76	−0.09	0.11	0.16	0.1	0.91–0.92
U	0.15	−0.09	2.36	0.05	0.1	0.39	0.91–0.97
Inbound							
P	0.63	0.1	0.13	0.46	0.12	0.04	0.83–0.89
F	0.1	0.7	0.01	0.12	0.09	0.13	0.85–0.90
U	0.13	0.01	1.96	0.04	0.13	0.21	0.89–0.94

The R^2 values represent the correlation coefficients of the multiple linear regression performed on the original (uncompensated) data.

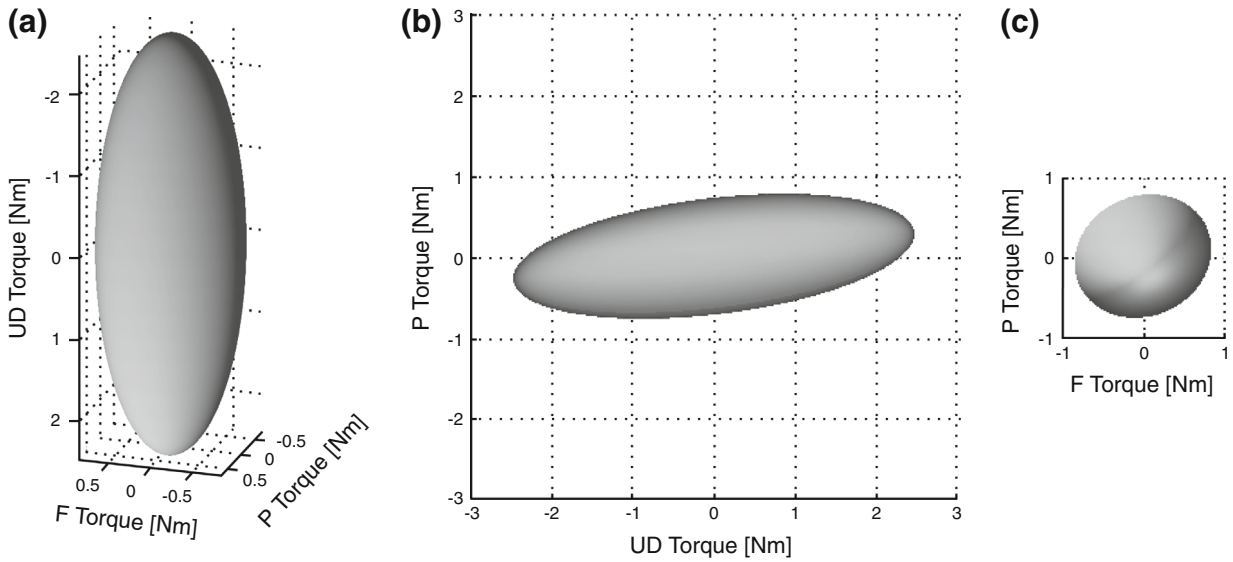

FIGURE 5. Mean stiffness ellipsoid and 2-dimensional projections for outbound movements, averaged over male and female subjects. (a) Isometric view. (b) Stiffness is significantly greater in RUD than in PS (and FE, not shown). (c) Stiffness is similar in FE and PS. Negative values of torque in pronation, flexion, and ulnar deviation represent torque in supination, extension, and radial deviation, respectively.

The difference in stiffness in different directions was also seen between PS, FE, and RUD, though not as markedly since differences between directions are always largest between the principal axes. Comparing diagonal elements of the stiffness matrices listed in Table 1, the average ratio of stiffness in PS to stiffness in RUD was 0.30 ± 0.052 (mean ± SD), the ratio of stiffness in FE to stiffness in RUD was 0.34 ± 0.019, and the ratio of the stiffness in PS to stiffness in FE was 0.89 ± 0.18.

The orientation of the major eigenvector pointed roughly in the direction of pure RUD for all subjects. The angle between the major eigenvector and the RUD axis was on average 8.47° ± 3.91° (Table 2), with no significant effects of direction or gender (Table 3). The direction of the major eigenvector forced the

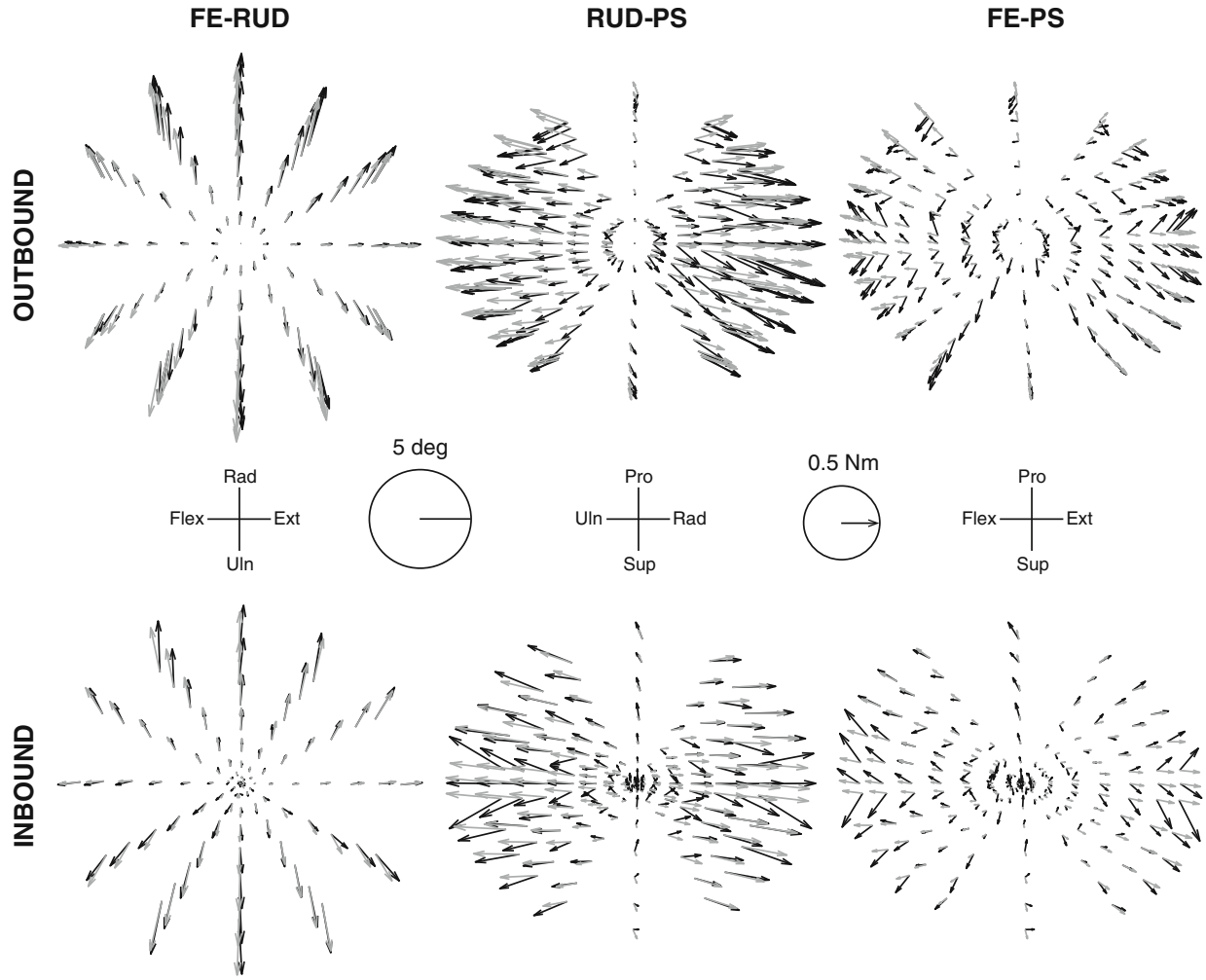

FIGURE 6. Comparison of the raw torque field measured from a single subject(black)and the torque field predicted at the same locations by that subject's stiffness matrix (gray). We used the subject's total stiffness matrix, i.e., the sum of the conservative (symmetric) and non-conservative (anti-symmetric) portions, but the torque field predicted by the conservative portion of the stiffness matrix is almost identical because the non-conservative portion is so small. Shown are torque fields measured during outbound and inbound movements (top and bottom row, respectively) to targets in the FE–RUD, RUD–PS, and FE–PS planes (left, middle, and right column, respectively). The directions in each plane are given by the compass roses between the top and bottom rows. Each arrow represents the torque measured or predicted at the location where the arrow originates. Scales for the locations and arrow lengths are given in terms of 5° and 0.5 N m, respectively.

TABLE 2. Ellipsoid shape, orientation, and volume by gender and direction (inbound vs. outbound).

	Min/Maj		Int/Maj		Angle (°)		Volume (N m/rad)^3	
	Mean	SD	Mean	SD	Mean	SD	Mean	SD
Male								
Outbound	0.22	0.08	0.37	0.07	8.4	2.83	9.11	4.89
Inbound	0.24	0.09	0.39	0.06	9.45	3.32	6.65	3.8
Female								
Outbound	0.19	0.11	0.48	0.17	8.54	5.1	6.4	6.2
Inbound	0.2	0.1	0.46	0.08	7.71	3.44	3.33	2.64

Shape is given as the ratio of eigenvalues (Maj, Int, and Min represent major, intermediate, and minor eigenvalues, respectively). Orientation is given as the angle between the major eigenvector and the RUD axis.

TABLE 3. *F* values and *p* values for main and interaction effects of direction and gender for the ANOVA tests performed for each dependent variable (defined in the caption to Table 2).

Dependent variable	Effect	$F_{1,8}$	p
Min/Maj	Direction	0.13	0.73
	Gender	0.01	0.91
	Direction*gender	0.17	0.69
Int/Maj	Direction	0.01	0.91
	Gender	0.61	0.46
	Direction*gender	0.34	0.57
Angle	Direction	0.00	0.95
	Gender	0.11	0.75
	Direction*gender	1.01	0.35
Volume	Direction	9.28	0.016*
	Gender	1.05	0.34
	Direction*gender	0.11	0.75

The difference in the volume of the stiffness ellipsoid between outbound and inbound movements was the only statistically significant effect ($p < 0.05$).

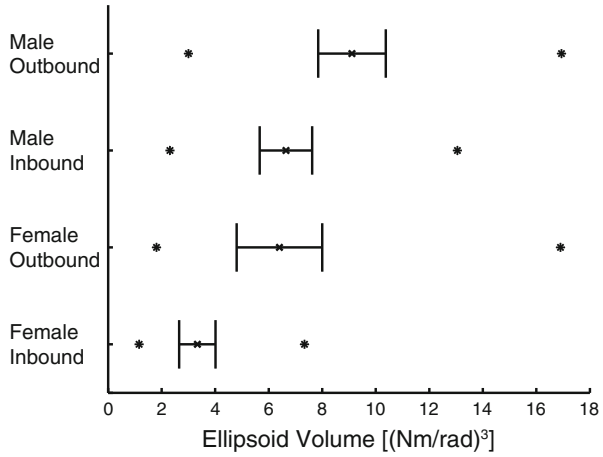

FIGURE 7. Mean, standard error, and range (minimum and maximum values) of the volume of stiffness ellipsoids by gender and direction (outbound vs. inbound). Note that reporting differences in stiffness magnitude by comparing differences in volume (as opposed to average magnitude, for example) emphasizes the differences because volume is proportional to the product of the three eigenvalues.

intermediate and minor eigenvectors to lie roughly in the FE–PS plane, with no significant correlation between the minor or the intermediate eigenvectors and the PS or FE axes, demonstrated by the finding that there was no significant difference ($p = 0.45$) between the angle formed by the minor eigenvector and PS axis and 45°, which is the angle expected for a random distribution. The findings that the major eigenvector aligned closely with the RUD axis but the intermediate and minor eigenvectors showed no consistent orientation imply that stiffness in FE and PS are similar even though the minor axis was, on average, half as large as the intermediate axis (see "Discussion" section).

The ellipsoid volume was significantly larger for outbound than for inbound movements ($F_{1,8} = 9.28$, $p = 0.016$, Table 3); the average volume for inbound movements was 64% of the volume for outbound movements. The average volume for female subjects was 62% of the volume for male subjects (Fig. 7), but the difference was not statistically significant (Table 3). Note that reporting differences in stiffness magnitude by comparing differences in volume emphasizes the differences because volume is proportional to the product of the eigenvalues; for example, while the average female volume is only 64% of the average male volume, the eigenvalues of the average female ellipsoid are 95, 85, and 77% as large as those of the average male ellipsoid.

DISCUSSION

Coordinated motor control requires that the neuromuscular system account and compensate for joint dynamics. Recent studies have shown that stiffness dominates wrist dynamics[8,9]; more specifically, wrist stiffness is anisotropic,[14] creating "paths of least resistance" which may be exploited by the neuromuscular system when it has the opportunity—for example, when the three DOF of the wrist and forearm are used to complete a task that only requires two DOF. Understanding how wrist and forearm rotations are coordinated requires an understanding of the stiffness encountered during combined wrist and forearm rotations. Here we have characterized the passive stiffness of coupled wrist and forearm rotations of 15° amplitude and found that the stiffness is highly anisotropic, with the major eigenvector approximately 5 times larger than the minor eigenvector and closely aligned with the RUD axis.

Comparison to Prior Measurements

Because this is the first-ever measurement of stiffness for combinations of PS, FE, and RUD, it is not possible to compare the entire 3-by-3 stiffness matrix to previous measurements. However, the elements of the stiffness matrix corresponding to stiffness in PS, FE, and RUD individually, and to FE and RUD combined, can be compared to previous measurements. The diagonal values of the stiffness matrices reported here represent the passive stiffness along the anatomical axes (PS, FE, and RUD). The mean stiffness in FE measured in this study (0.85 N m/rad) is in good agreement with prior studies, falling in the middle of previous measurements, which range from 0.15 to 3 N m/rad.[12,25] Our mean stiffness measurement in RUD (2.47 N m/rad) is higher than the two previous

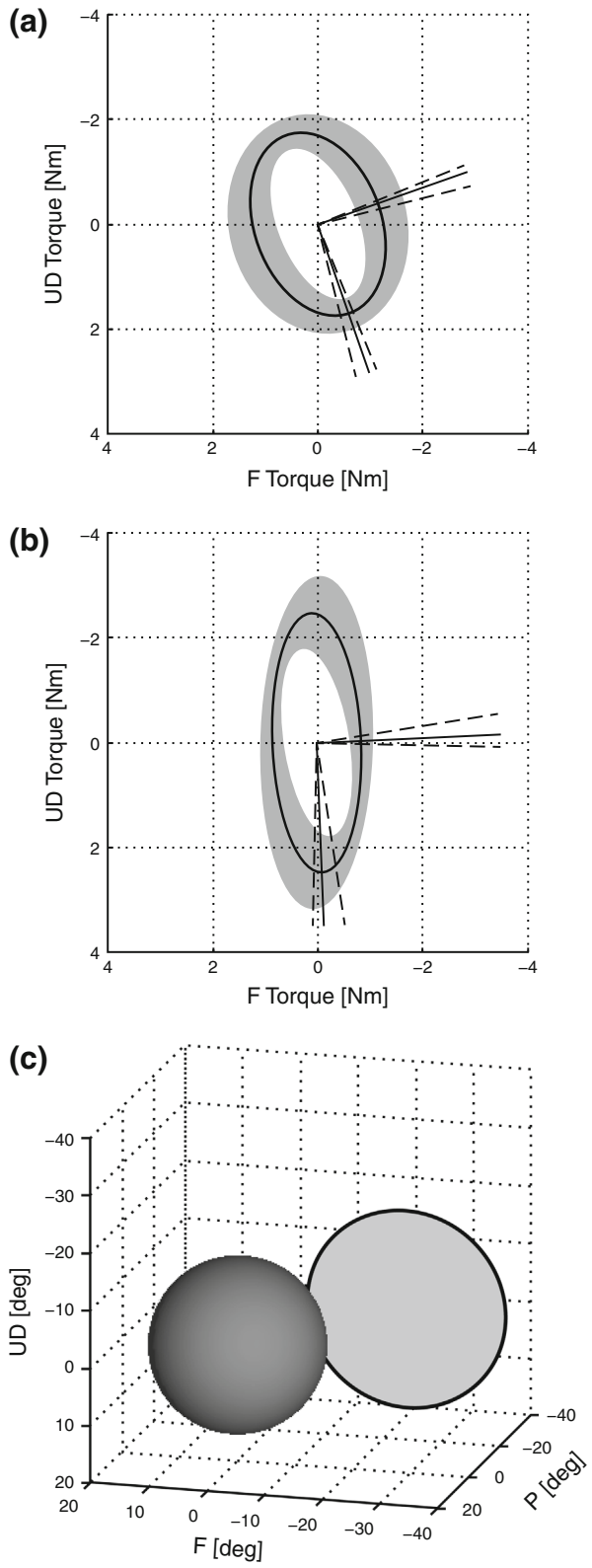

FIGURE 8. Comparison of the FE–RUD portion of our stiffness measurement (which also included PS) to the only prior stiffness measurement in FE and RUD.[14] Mean stiffness ellipse in FE–RUD for (a) the current study and (b) the prior 2-DOF study.[14] The line represents the mean ellipse, and the inside and outside border of the shaded region represent the ellipses of the mean ± 1 standard deviation matrices. Also shown are the principal axes of each ellipse (the solid axes are for the average matrix, and the dashed axes for the mean ± 1 standard deviation matrices). (c) Differences in the origin of the stiffness measurements between the current study and the prior 2-DOF study.[14] The measurement space in the current (3-DOF) study is represented by the sphere and is centered in neutral anatomical position (shown here at the origin of PS–FE–RUD space). The measurement space in the prior 2-DOF study[14] is represented by the circle (contained in an FE–RUD plane) and is centered at approximately −34°, −20°, and 1.5° in pronation, flexion, and ulnar deviation, respectively.

measurements of passive stiffness in RUD: 1.45 and 1.74 N m/rad.[14,28] Likewise, our mean value of stiffness in PS (0.74 N m/rad) is greater than the only previously published values of 0.19 N m/rad in pronation and 0.24 N m/rad in supination.[14] Only one previously reported study investigated passive wrist stiffness in directions involving both FE and RUD.[14] We compared the stiffness ellipse from that study with the stiffness ellipse obtained from the FE–RUD portion of our 3-DOF stiffness matrix and found good agreement, with the following minor differences (Figs. 8a and 8b): our FE-RUD ellipse is more anisotropic and more aligned with the FE–RUD axes. The ratio of minor to major eigenvector was 0.34 in our study compared to 0.68 in the previous study, and the angle between the major eigenvector and the RUD axis was 2.2° ± 4.1° in our study compared to 21° ± 9.2° in the previous study.

We believe the differences in stiffness between this study and the two prior studies reporting stiffness in RUD[28] or FE and RUD[14] were caused by the following, deliberate methodological differences. First, we defined the origin to be in neutral wrist and forearm position[32] to allow for general application to future studies. In contrast, in the previous studies, the origin was defined with the upper limb in a typical posture for grasping a handle (Fig. 8c). For example, in the prior two studies, the shoulder was abducted by approximately 40°, effectively supinating the forearm by 40°.[14] Rotating the forearm was recently shown to counter-rotate the pulling directions of the wrist muscles by 12% relative to a frame intrinsic to the wrist,[11] suggesting that the orientation of the ellipse in the study by Formica *et al.* was pronated by approximately 5° relative to the present study. Also, in the previous studies the origin in PS was determined by the orientation of the forearm when the hand was grasping the vertically oriented robot handle. We measured this alternate position in six of the subjects from the present study and found that grasping the handle pronated the forearm by 6.1° ± 3.2° compared to our neutral position. In FE and RUD, the origin was defined by the handle, which was inclined relative to the

horizontal plane by 17° and in line with the forearm in the parasagittal plane, forcing the wrist into an extended position. Compared to our study, this origin was in 20° ± 4° of extension and 2° ± 5° of ulnar deviation. Second, robot dynamics and gravitational effects added a substantial amount of apparent stiffness, meriting great care in estimating and removing their contribution. Here we went beyond the efforts of the previous two studies by estimating these effects separately for each subject based on each subject's hand mass and neutral position. Third, we are comparing the 1-DOF and 2-DOF stiffness estimates from the previous studies to a subset of the 3-DOF matrix from the present study. Because this subset came from a linear regression across the entire 3-DOF space, it is influenced by more DOF and is therefore not as specific to the 1-DOF or 2-DOF space as the previous measurements. Fourth, in the previous studies, the fingers were constrained in a flexed position around a handle, while we deliberately chose to the fingers to be unconstrained to encourage finger and wrist muscles to fully relax.

Limitations of This Study

As presented in the "Results" section, we found that the intermediate and minor axes lay roughly in the FE–PS plane but did not have any consistent orientation within that plane despite a 2:1 difference in their lengths. In other words, subjects exhibited one direction twice as stiff as the other, but the orientation of those directions was effectively random by subject. This large difference between subjects despite otherwise stereotyped shape and orientation likely reflects the fact that most of the torque in PS was devoted to overcoming gravitational effects (Fig. 4) and the stiffness in that direction is more variable than the stiffness in other directions, especially where PS stiffness was small (compare standard deviations and R^2 values between PS and FE for female subjects in Table 1).

Although care was taken to align the wrist and robot axes, they were not perfectly aligned. As explained in the "Methods" section, the location of the robot's differential gear mechanism forced an offset between the parallel FE axes of the wrist and robot of approximately 2 cm. Furthermore, while the robot was deliberately designed to allow for the offset of approximately 8 cm between the parallel RUD axes of the wrist and robot, the RUD angle recorded by the robot is not exactly the same as the RUD angle of the wrist. A theoretical analysis showed that an RUD displacement of the robot from −15° to 15° produced a displacement of the wrist from −13° to 19°, despite near perfect agreement close to the robot's neutral position.[6] While we believe the effect of these misalignments on average stiffness to be relatively small, further experimentation and analysis are required to quantify it exactly. We note that our stiffness measurement compares favorably to prior measurements performed under different experimental conditions: our stiffness in FE falls in the middle of prior measurements (see above). It is not possible to ascertain from prior studies the effect of this axis offset on stiffness in RUD because all prior measurements of stiffness in RUD were performed using the same robot. The effect in PS is expected to be minimal since the alignment of the PS axes of the forearm and robot is independent of the proximodistal location of the wrist joint.

Although the mean difference in magnitude between the measured and predicted torques was small (9.6, 28, and 10% for the whole, near, and far regions, respectively), the standard deviation was very large (69, 58, and 73%). The small mean and large standard deviation reflect the fact that the stiffness matrix is the optimal linear approximation of a phenomenon that is non-linear. Non-linearities in the measured stiffness can be seen in some of the torque fields shown in Fig. 6. For example, the torque measured during outbound movements to targets in the FE–PS plane (black arrows in the plot in the third column of the top row)cannot be perfectly fit by a linear torque–displacement relationship (i.e., constant stiffness matrix); such a relationship requires, among other characteristics, symmetry about the origin, which is clearly violated in some directions. The FE–PS plane appears to have the largest difference between measured and predicted torque, and therefore the greatest non-linearity in stiffness. This is likely because this plane has the smallest stiffness and the greatest torques due to gravity and robot dynamics (see Figs. 3 and 4), and therefore the smallest signal-to-noise ratio.

In general, the non-linearity of joint stiffness is complex and includes hysteresis,[14] short-range stiffness,[3,5] thixotropy,[3] asymmetry,[14] and other factors. While many studies will be required to fully characterize the non-linearities of coupled wrist and forearm movements, prior studies provide an estimate of the magnitude of these non-linearities in 1 or 2 DOF. Hysteresis in movements involving both FE and RUD was reported by Formica *et al.*[14] Their plots of torque vs. displacement show a relatively linear relationship when the wrist is passively rotated in a single direction (e.g., from a flexed to an extended position, or vice versa), but a sudden change in torque upon reversal of the movement direction. The magnitude of this change has not been characterized. Axelson and Hagbarth[3] investigated short-range stiffness and thixotropy, which is stiffness that depends on the immediately

preceding history of movement and contraction. Stiffness over the first 2° of movement was on the order of 1.5–4 times larger than stiffness after the first 2°, but this short-range stiffness decreased by approximately 20% during immediately succeeding movements and reappeared after a rest period of approximately 15 s, indicating that the first movement temporarily "limbers up" the joint. Formica *et al.*[14] also characterized asymmetry, reporting statistically significant differences in stiffness between flexion and extension and between radial and ulnar deviation, but not between pronation and supination. They found stiffness in extension to be 1.8 times greater than stiffness in flexion, and stiffness in radial deviation to be 1.4 times greater than stiffness in ulnar deviation. However, note that stiffness asymmetry is highly dependent on the choice of neutral position, which was located in 20° of extension compared to the current study.

Since the stiffness of coupled wrist and forearm movements has never been characterized in linear or non-linear form, the purpose of this study was to provide the first and most fundamental approximation, which is a linear approximation. While this approximation is not accurate at predicting the measured torque at any one location, on average it predicts torque quitewell, with a 9.6% error in magnitude and 3.6° error in angle over the entire range measured (±15° in all directions). Considering only the near (<7.5°) or far (>7.5°) ranges, the mean errors in magnitude (28 and 10%) and angle (12° and 1.2°) are still relatively small, especially compared to the 20-fold range of previously measured stiffness values mentioned above.

Implications for the Neural Control of Movement

The anisotropy in stiffness creates a control challenge because it causes path curvature unless the muscular activation patterns specifically compensate for the anisotropy.[7,9] The difference between RUD and FE measured here (ratio of 0.34) is approximately twice as great as previously reported and would result in more path curvature, and a greater control challenge for making straight paths, than previously thought.[9] The difference between RUD and PS was equally large (ratio of 0.30).

The coupling between PS and RUD produces significant interaction due to stiffness between these DOF. On average, it requires only 4° of displacement in RUD to produce as much torque in PS as 1° of displacement in PS (compare the [1,3] and [1,1] elements of the stiffness matrices in Table 1). The coupling between FE and RUD reported here, which was measured as the angle between the principal stiffness axes and the anatomical axes to be 2°, is smaller than the previously reported value of 21°.[14] From the point of view of neural control, the amount of coupling between FE and RUD is not critically important because almost all wrist movements involve both FE and RUD and therefore require torques in both DOF anyway. The large variability in the magnitude of stiffness (ellipsoid volume) between subjects is similar to the large variability in body segment inertia and has been discussed previously.[14]

As mentioned in the introduction, the anisotropy in wrist stiffness creates paths of least resistance which could be exploited by using PS to orient the wrist to use FE instead of RUD, assuming the stiffness in PS is small enough to make this substitution worthwhile. Here we have shown that the stiffness in PS is significantly smaller than the stiffness in RUD, indicating that the torque required to move in combinations of PS and FE is significantly smaller than the torque required to move in combinations of FE and RUD (assuming equal displacements). The coupled stiffness measured here will enable future research to determine optimal paths and to compare these optimal paths to observed movements involving wrist and forearm rotations.

ACKNOWLEDGMENTS

We'd like to thank Dr. Dennis Eggett (BYU Statistical Consulting Center) for technical assistance with the statistical analysis.

REFERENCES

[1]An, K.-N., R. A. Berger, and W. P. I. Cooney (eds.). Biomechanics of the Wrist Joint. New York: Springer, p. 42, 1991.
[2]Anderton, W. and S. Charles. Kinematic coupling of wrist and forearm movements. In: Annual Meeting of the American Society of Biomechanics, Gainesville, FL, 2012.
[3]Axelson, H. W., and K. E. Hagbarth. Human motor control consequences of thixotropic changes in muscular short-range stiffness. *J. Physiol. Lond.* 535(1):279–288, 2001.
[4]Berens, P. CircStat: a MATLAB toolbox for circular statistics. *J. Stat. Softw.* 31(10):1–21, 2009.
[5]Campbell, K. S. Short-range mechanical properties of skeletal and cardiac muscles. In: Muscle Biophysics: From Molecules to Cells, edited by D. E. Rassier. New York: Springer, 2010, pp. 223–246.
[6]Celestino, J. Characterization and control of a robot for wrist rehabilitation. MS, Massachusetts Institute of Technology, 2003, p. 128.
[7]Charles, S. K., and N. Hogan. The curvature and variability of wrist and arm movements. *Exp. Brain Res.* 203(1):63–73, 2010.
[8]Charles, S. K., and N. Hogan. Dynamics of wrist rotations. *J. Biomech.* 44(4):614–621, 2011.

[9]Charles, S. K., and N. Hogan. Stiffness, not inertial coupling, determines path curvature of wrist motions. *J. Neurophysiol.* 107:1230–1240, 2012.
[10]de Leva, P. Adjustments to Zatsiorsky–Seluyanov's segment inertia parameters. *J. Biomech.* 29(9):1223–1230, 1996.
[11]de Rugy, A., R. Davoodi, and T. J. Carroll. Changes in wrist muscle activity with forearm posture: implications for the study of sensorimotor transformations. *J. Neurophysiol.* 108(11):2884–2895, 2012.
[12]De Serres, S. J., and T. E. Milner. Wrist muscle activation patterns and stiffness associated with stable and unstable mechanical loads. *Exp. Brain Res.* 86:451–458, 1991.
[13]Dolan, J. M., M. B. Friedman, and M. L. Nagurka. Dynamic and loaded impedance components in the maintenance of human arm posture. *IEEE Trans. Syst. Man Cybern.* 23(3):698–709, 1993.
[14]Formica, D., S. K. Charles, L. Zollo, E. Guglielmelli, N. Hogan, and H. I. Krebs. The passive stiffness of the wrist and forearm. *J. Neurophysiol.* 108:1158–1166, 2012.
[15]Fung, Y. Biomechanics: Mechanical Properties of Living Tissues. New York: Springer, 1993.
[16]Gehrmann, S. V., R. A. Kaufmann, and Z. M. Li. Wrist circumduction reduced by finger constraints. *J. Hand Surg. Am.* 33(8):1287–1292, 2008.
[17]Gielen, C., and J. C. Houk. Nonlinear viscosity of human wrist. *J. Neurophysiol.* 52(3):553–569, 1984.
[18]Given, J. D., J. P. A. Dewald, and W. Z. Rymer. Joint dependent passive stiffness in paretic and contralateral limbs of spastic patients with hemiparetic stroke. *J. Neurol. Neurosurg. Psychiatry* 59(3):271–279, 1995.
[19]Hogan, N. The mechanics of multi-joint posture and movement control. *Biol. Cybern.* 52:315–331, 1985.
[20]Hollerbach, J. M., and T. Flash. Dynamic interactions between limb segments during planar arm movement. *Biol. Cybern.* 44(1):67–77, 1982.
[21]Ives, J. C., and J. K. Wigglesworth. Sampling rate effects on surface EMG timing and amplitude measures. *Clin. Biomech.* 18(6):543–552, 2003.
[22]Krebs, H., B. T. Volpe, D. Williams, J. Celestino, S. Charles, D. Lynch, and N. Hogan. Robot-aided neurorehabilitation: a robot for the wrist rehabilitation. *IEEE Trans. Neural Syst. Rehabil. Eng.* 15(3):327–335, 2007.
[23]Lariviere, C., A. Delisle, and A. Plamondon. The effect of sampling frequency on EMG measures of occupational mechanical exposure. *J. Electromyogr. Kinesiol.* 15(2):200–209, 2005.
[24]Leger, A. B., and T. E. Milner. Passive and active wrist joint stiffness following eccentric exercise. *Eur. J. Appl. Physiol.* 82(5–6):472–479, 2000.
[25]Lehman, S. L., and B. M. Calhoun. An identified model for human wrist movements. *Exp. Brain Res.* 81(1):199–208, 1990.
[26]Mussa-Ivaldi, F. A., N. Hogan, and E. Bizzi. Neural, mechanical, and geometric factors subserving arm posture in humans. *J. Neurosci.* 5(10):2732–2743, 1985.
[27]Ochi, E., K. Nakazato, and N. Ishii. Effects of eccentric exercise on joint stiffness and muscle connectin (titin) isoform in the rat hindlimb. *J. Physiol. Sci.* 57(1):1–6, 2007.
[28]Rijnveld, N. and H. I. Krebs. Passive wrist joint impedance in flexion–extension and abduction-adduction. In: International Conference on Rehabilitation Robotics, Noordwijk, Netherlands, 2007.
[29]Whitehead, N. P., D. L. Morgan, J. E. Gregory, and U. Proske. Rises in whole muscle passive tension of mammalian muscle after eccentric contractions at different lengths. *J. Appl. Physiol.* 95(3):1224–1234, 2003.
[30]Whitehead, N. P., N. S. Weerakkody, J. E. Gregory, D. L. Morgan, and U. Proske. Changes in passive tension of muscle in humans and animals after eccentric exercise. *J. Physiol.* 533(Pt 2):593–604, 2001.
[31]Williams, D. A Robot for Wrist Rehabilitation. MS, Massachusetts Institute of Technology, 2001, p. 59–62.
[32]Wu, G., F. C. T. van der Helm, H. E. J. Veeger, M. Makhsous, P. Van Roy, C. Anglin, J. Nagels, A. R. Karduna, K. McQuade, X. G. Wang, F. W. Werner, and B. Buchholz. ISB recommendation on definitions of joint coordinate systems of various joints for the reporting of human joint motion—Part II: shoulder, elbow, wrist and hand. *J. Biomech.* 38(5):981–992, 2005.